

A Plasma Torus Around a Young Low-Mass Star

Luke G. Bouma^{1,2}

¹*Observatories of the Carnegie Institution for Science, Pasadena, CA 91101, USA*

²*Carnegie Fellow*

Approximately one percent of red dwarfs younger than 100 million years show structured, periodic optical light curves suggestive of transiting clumps of opaque circumstellar material that corotate with the star^{1–4}. The composition, origin, and even the existence of this material are uncertain. The main alternative hypothesis is that these stars are explained by complex distributions of dark starspots or bright faculae distributed across their surfaces⁵. Here, we present time-series spectroscopy and photometry of a 40 million year old complex periodic variable (CPV), TIC 141146667. The spectra show coherent sinusoidal Balmer emission at up to four times the star’s equatorial velocity, demonstrating the presence of extended clumps of circumstellar plasma — a plasma torus. Given that long-lived condensations of cool (10^4 K) plasma can persist in the hot (10^6 K) coronae of stars with a wide range of masses^{6–11}, these data support the idea that such condensations can become optically thick around the lowest-mass stars, although the exact source of opacity remains unclear.

1 Main

M dwarfs, stars with masses below about half that of the Sun, are the only type of star to offer near-term prospects for detecting the atmospheres of rocky exoplanets with water on their surfaces (CITE). Investment with JWST has proceeded accordingly (CITE CITE). It is therefore important to consider how the evolution of an M dwarf might impact the evolution of its planets. Previous work has established that most M dwarfs host close-in planets (CITE), and that these planets are often subject to long circumstellar disk lifetimes (CITE), to large doses of UV radiation (CITE), and to a high incidence of flares and coronal mass ejections (CITE). However, despite excellent work in these areas, the properties of the circumstellar plasma and magnetospheric environments to which young, close-in exoplanets are subject remain largely unexplored.

One glaring example of our current ignorance is the complex periodic variables (CPVs). Figure 1 highlights the main object of interest in this article, but over one hundred analogous objects have now been discovered by K2 and TESS (CITE, CITE, CITE, CITE). These CPVs are defined by their highly structured and periodic optical light curves, and most are M dwarfs with rotation periods shorter than two days. Within current sensitivity limits, none have primordial disks (CITE). However, $\approx 3\%$ of stars a few million years old show this behavior (CITE), and the observed fraction decreases to $\approx 0.3\%$ by ≈ 150 Myr (CITE).

The two leading hypotheses to explain the CPVs are either that transiting clumps of circumstellar material corotate with the star (CITE, CITE, CITE), or that these stars represent an extreme

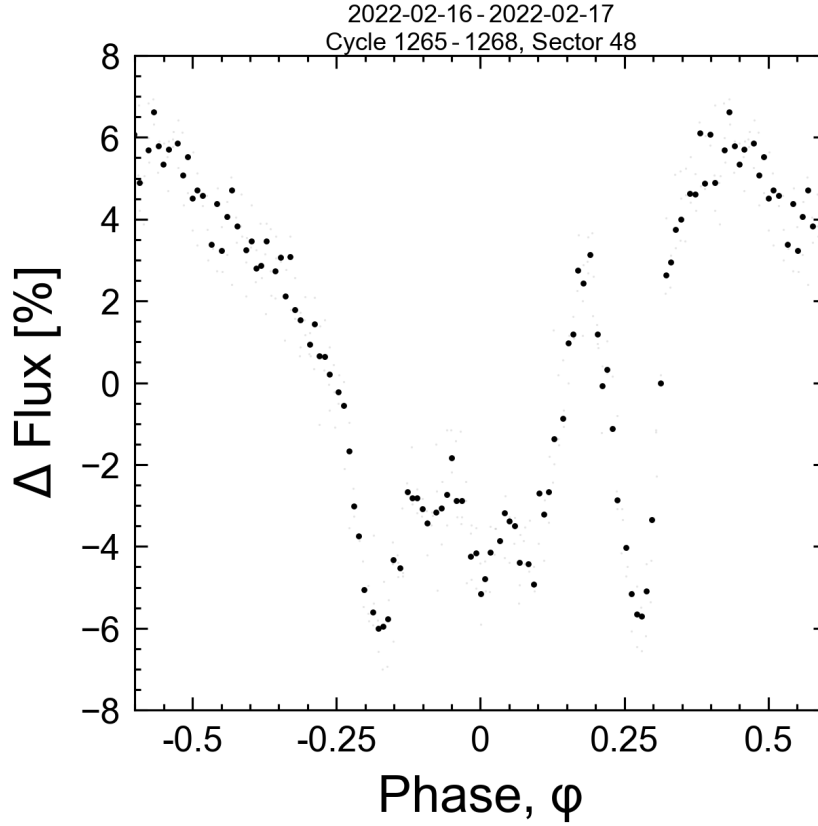


Figure 1: **Figure 1 (Movie): TIC 141146667 is a complex periodic variable (CPV).** For the best experience, please view the online movie available [here](#), which spans a baseline of 5,784 cycles irregularly sampled over three years. The TESS light curve is phased to the 3.930 hour period in groups of a few cycles per frame. This is the period both of stellar rotation, and (we hypothesize) of corotating clumps of circumstellar material. Raw data acquired with two minute sampling are in gray; black is their average. Similar to other members of this class, the sharp photometric features persist for tens to thousands of rotational cycles.

in naturally-occurring distributions of starspots or faculae for young M dwarfs⁵. Currently, the main argument against a starspot-only explanation invokes the timescales and amplitudes of the sharpest photometric features (CITE). However, no independent evidence has yet been presented for the presence of circumstellar material in these objects. Since transiting circumstellar clumps would geometrically imply an occurrence rate a few to ten times the observed rate (CITE), the question of whether it is there could potentially teach us about 10-30% of M dwarfs during their early lives.

The dearth of evidence for circumstellar material around CPVs is surprising given that separate studies of young BAFGKM stars have, for decades, reported that stellar coronae contain both

hot (10^6 K) and cool (10^4 K) plasma. In particular, time-series spectroscopy has shown periodic high-velocity absorption and emission in Balmer lines such as $H\alpha$, caused by long-lived, corotating clumps of cool plasma (CITE, CITE, CITE). Such clumps are forced into corotation by the magnetic field, and the exact geometry of where the plasma can accumulate is dictated by the magnetic field's topology. For instance, a tilted dipole field tends to yield an accumulation surface of a warped torus ⁷, whereas in the limit of a single strong discrete field line, accumulation occurs along a fixed point ¹⁰. However, none of these stars have shown any photometric anomalies (CITE), leaving open the issue of whether these two separate areas of study have any direct connection. Nonetheless, CPVs do respond to sudden magnetic field changes: there are many documented cases of otherwise long-lived eclipse features disappearing immediately following stellar flares (CITE, CITE).

In this study, we present the first observations of corotating clumps of cool plasma around a CPV. We identified TIC 141146667 in previous work ⁴ by searching the TESS two-minute data for stars showing periodic variability with at least three sharp dips per cycle. We selected it from the resulting fifty high-quality CPVs for spectroscopic observations because it was the brightest source for which a full cycle could be observed in a half-night. We observed it for five hours on UT 2024-02-17 using the High Resolution Echelle Spectrometer (HIRES; ¹²) on the Keck I 10m telescope, roughly contemporaneous with TESS, which observed the star from UT 2024-02-05 to UT 2024-02-26 with a duty cycle of XX%. In detail, TESS was finishing a data downlink during the HIRES observations, and photometric data collection resumed three rotation cycles (12 hours) after the spectra were acquired. Extended Data Figure 1 shows the detailed photometric behavior of the star before and after the exact epoch of observation; the star remained sufficiently stable to not affect any of the interpretation that follows.

Results Figure 2 shows the data from February 2024. As expected based on other CPVs ⁴, the photometric shape of TIC 141146667 evolved over the years following the 2022 discovery data, while nonetheless remaining complex. In February 2024, the average photometric signal showed a gradual brightening over 45% of the period, followed by a complex eclipse-like feature spanning 55% of the period. This eclipse-like feature shows two to three local photometric minima, and one to two local maxima.

The spectroscopy shows emission well outside the star's equatorial velocity ($v_{\text{eq}}=130 \text{ km s}^{-1}$). There are at least two distinct emission components, each spaced half a cycle apart in phase. The first has clearer sinusoidal behaviour and is double-peaked, with semi-amplitudes of $K_1=2.1 v_{\text{eq}}$ and $2.7 v_{\text{eq}}$. The flux excesses from these two peaks are correlated with one another, with amplitudes varying from 100% of the continuum flux early in the observation sequence to 30% by its end. The component 180° opposite in phase is only detected from $\phi=0.2$ -1.0, and from $\phi=0.2$ -0.5, this latter component appears connected to the star in velocity space. While its peak semi-amplitude of $K_1=3.9 v_{\text{eq}}$ is achieved at both $\phi=0.25$ and 0.75 , its amplitude decreases from a 60% excess beyond the continuum to a 10% excess. The sinusoidal period in all cases where emission is seen is consistent with the photometric 3.930 hour period. As we shall discuss below, the only plausible

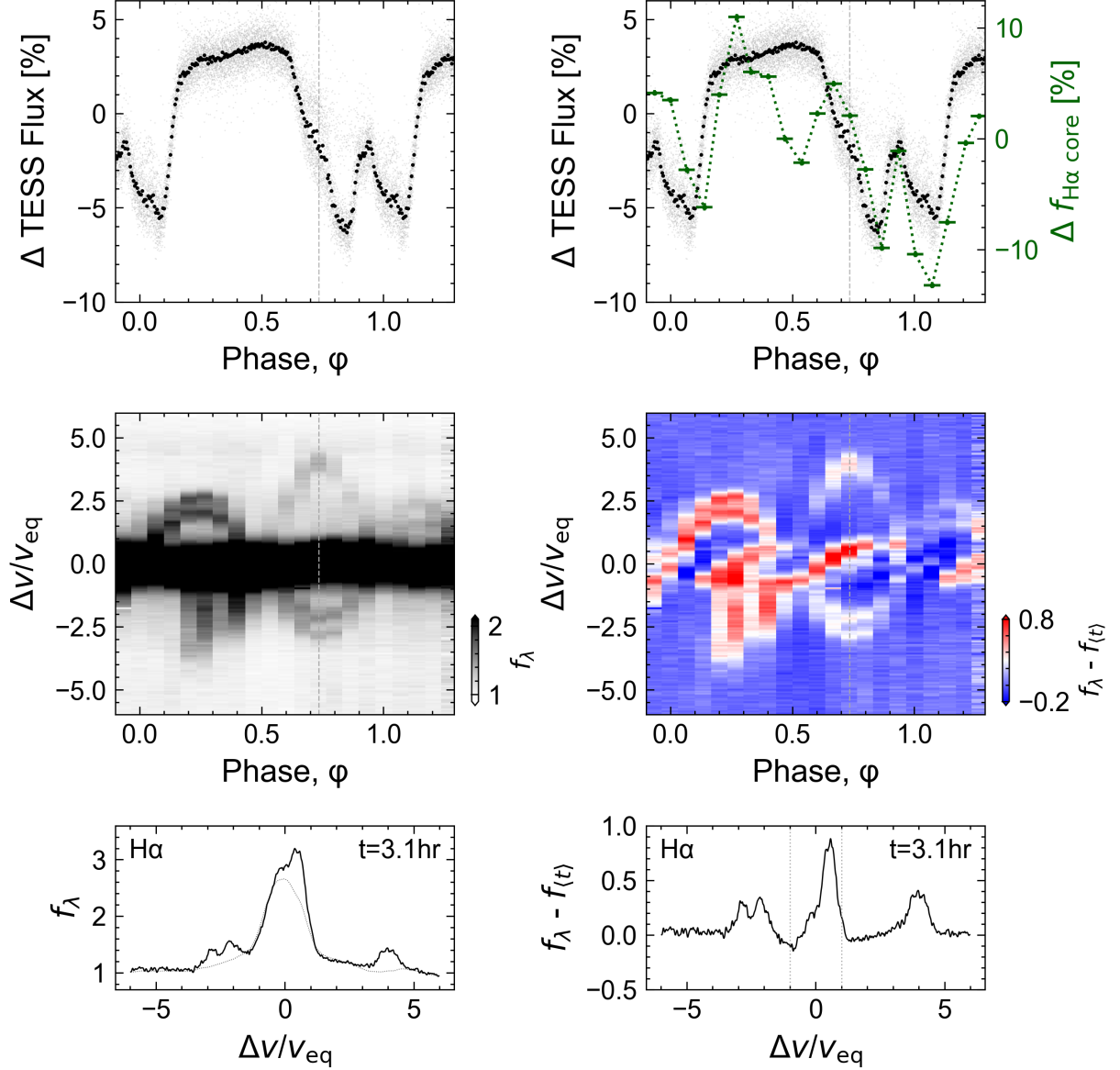


Figure 2: **Figure 2 (Movie):** Hydrogen emission from circumstellar plasma orbiting TIC 141146667. **(TODO)**For the best experience, please view the online movie available here. **Panel a:** TESS light curve from UT 2024-02-05 to UT 2024-02-26 folded on the 3.930 hour period. Black points are averaged; gray are the raw data. **Panel b:** Keck/HIRES H α spectra acquired on UT 2024-02-17. The continuum is set to unity, and the darkest color is set at twice the continuum to accentuate emission outside the line core ($|v/v_{\text{eq}}| > 1$, for $v_{\text{eq}}=130 \text{ km s}^{-1}$). While emission in the line core originates in the stellar chromosphere, the sinusoidal emission features are most readily described by a warped plasma torus. **Panel c:** Individual epochs of Panel b, visible in the online movie. The dotted line shows a time-averaged spectrum, $f_{(t)}$. **Panel d:** As in Panel a, but overplotting the median-normalized H α light curve at $|v/v_{\text{eq}}| < 1$. **Panel e:** As in Panel b, after subtracting the time-averaged spectrum. In addition to circumstellar emission, the line core shows absorption during the plasma clump transits. The asymmetric stretch is set to match the dynamic range of the data. **Panel f:** Individual epochs of Panel e, visible in the online movie.

explanation for the behavior at $|\Delta v/v_{\text{eq}}| > 1$ is that circumstellar clumps of hydrogen are corotating with the star. These clumps transit in front of the star when passing from negative to positive velocity.

Within the stellar $\text{H}\alpha$ line core, at $|\Delta v/v_{\text{eq}}| < 1$, the behavior is more complex. Generally, one would expect this region to be generated by the net superposition of bright and dark regions on the stellar surface, and then modulated by any occulting material capable of absorbing or emitting in $\text{H}\alpha$. In Figure 2e, the behavior from $\phi=0.4$ -1.2, is most easily interpreted: from $\phi=0.4$ -0.9, a hot region first gradually crosses the stellar line profile, following from $\phi=0.7$ -1.2 by the transit of a cool region. The phases $\phi < 0.4$ seem to be a mix of similar events, though the time sampling is sufficiently coarse that the interpretation is less clear. A final exercise to quantify the behavior in the line core is shown in Figure 2d, where $f_{\text{H}\alpha \text{ core}}$ denotes the summed flux in the at $|\Delta v/v_{\text{eq}}| < 1$. Changes in the line core flux are usually correlated with the broadband variability, except at $\phi=0.5$, during the transit of the higher-velocity clump and the occultation of the lower-velocity clump.

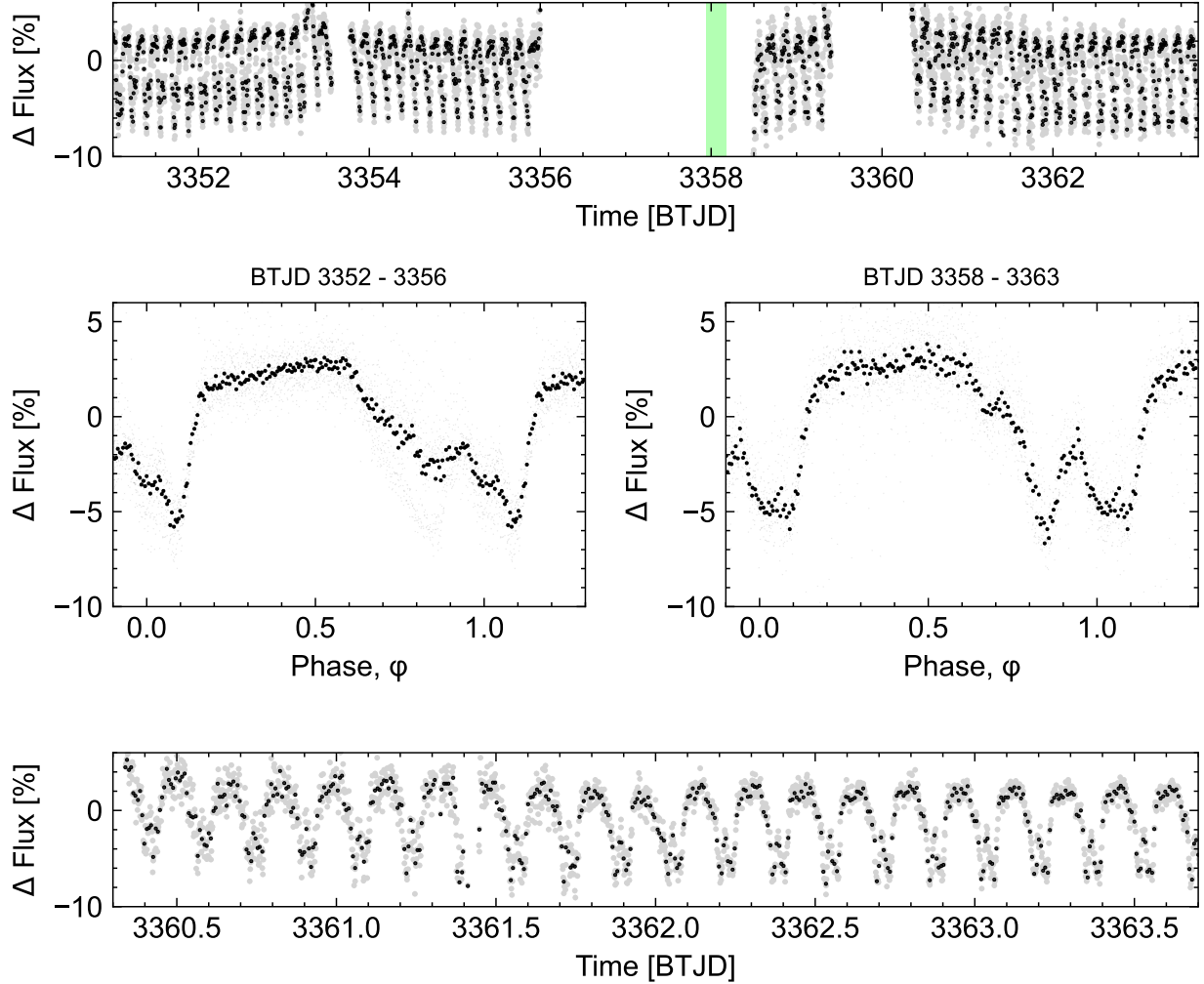
Discussion These data rule out “starspot-only” and “dust-only” origin scenarios for CPVs, instead supporting either a purely stellar origin for the phenomenon or extrinsic scenarios involving long-lived disks or outgassing rocky bodies capable of supplying sufficient gas.

- From self-shielding: find $n_{\text{H}} \sim f \cdot 10^{10} \text{ cm}^{-3}$. - What about from the *equivalent width* of the emission?

Methods

Observations TESS:

Keck/HIRES: We observed using the standard setup and reduction techniques of the California Planet Survey¹³. Winds of 30 mph contributed to $1''.2 \pm 0''.2$ seeing over the spectroscopic observations.



Extended Data Figure 1: Detailed photometric evolution of TIC 141146667 near the epoch of spectroscopic observation (green). **Panel a:** Subset of TESS SAP_FLUX acquired near time of Keck/HIRES observation. TESS downlinked data to the Deep Space Network from BTJD XXX to YYY, and was affected by scattered light from the Earth from BTJD 3359.4 to 3360.15. **Panels b,c:** Folded light curve before and after spectroscopy. **Panel d:** Zoom-in of Panel a, showing decreasing photometric scatter in the over three days (18 cycles).

Data Reduction

1. Rebull, L. M. *et al.* Rotation in the Pleiades with K2. II. Multiperiod Stars. *Astron. J.* **152**, 114 (2016).
2. Stauffer, J. *et al.* Orbiting Clouds of Material at the Keplerian Co-rotation Radius of Rapidly Rotating Low-mass WTTs in Upper Sco. *Astron. J.* **153**, 152 (2017).
3. Rebull, L. M. *et al.* Rotation of Low-mass Stars in Upper Scorpius and ρ Ophiuchus with K2. *Astron. J.* **155**, 196 (2018).
4. Bouma, L. G. *et al.* Transient Corotating Clumps around Adolescent Low-mass Stars from Four Years of TESS. *Astron. J.* **167**, 38 (2024).
5. Koen, C. Starspot modelling of the TESS light curve of CVSO 30. *Astron. Astrophys.* **647**, L1 (2021).
6. Collier Cameron, A. & Robinson, R. D. Fast H-alpha variations on a rapidly rotating cool main sequence star- I. Circumstellar clouds. *Mon. Not. R. Astron. Soc.* **236**, 57–87 (1989).
7. Townsend, R. H. D. & Owocki, S. P. A rigidly rotating magnetosphere model for circumstellar emission from magnetic OB stars. *Mon. Not. R. Astron. Soc.* **357**, 251–264 (2005).
8. Dunstone, N. J., Collier Cameron, A., Barnes, J. R. & Jardine, M. The coronal structure of Speedy Mic - II. Prominence masses and off-disc emission. *Mon. Not. R. Astron. Soc.* **373**, 1308–1320 (2006).
9. Petit, V. *et al.* A magnetic confinement versus rotation classification of massive-star magnetospheres. *Mon. Not. R. Astron. Soc.* **429**, 398–422 (2013).
10. Waugh, R. F. P. & Jardine, M. M. Magnetic confinement of dense plasma inside (and outside) stellar coronae. *Mon. Not. R. Astron. Soc.* **514**, 5465–5477 (2022).
11. Daley-Yates, S. & Jardine, M. M. Simulating stellar coronal rain and slingshot prominences. *Mon. Not. R. Astron. Soc.* **534**, 621–633 (2024).
12. Vogt, S. S. *et al.* *SPIE Conference Series*, vol. 2198 (1994).
13. Howard, A. W. *et al.* The California Planet Survey. I. Four New Giant Exoplanets. *Astrophys. J.* **721**, 1467–1481 (2010).

Parameter	Host	Source
Identifiers		
TIC	141146667	TESS
Gaia	todo	Gaia DR3
Astrometry		
α	todo	Gaia DR3
δ	todo	Gaia DR3
μ_α (mas yr ⁻¹)	todo	Gaia DR3
μ_δ (mas yr ⁻¹)	todo	Gaia DR3
π (mas)	todo	Gaia DR3
Photometry		
<i>TESS</i> (mag)	todo	TESS
<i>G</i> (mag)	todo	Gaia DR3
<i>G</i> _{BP} (mag)	todo	Gaia DR3
<i>G</i> _{RP} (mag)	todo	Gaia DR3
<i>J</i> (mag)	todo	2MASS
<i>H</i> (mag)	todo	2MASS
<i>K_s</i> (mag)	todo	2MASS
<i>W1</i> (mag)	todo	ALLWISE
<i>W2</i> (mag)	todo	ALLWISE
<i>W3</i> (mag)	todo	ALLWISE
<i>W4</i> (mag)	todo	ALLWISE
Kinematics and Position		
<i>RV_{Bary}</i> (km s ⁻¹)	13.35 ± 3.39	Gaia DR3
<i>U</i> (km s ⁻¹)		
<i>V</i> (km s ⁻¹)		
<i>W</i> (km s ⁻¹)		
<i>X</i> (pc)		
<i>Y</i> (pc)		
<i>Z</i> (pc)		
Physical Properties		
<i>P_{rot}</i> (hours)	3.930 ± 0.XXX	This work
<i>v</i> sin <i>i</i> _★ (km s ⁻¹)	todo	This work
<i>i</i> _★ (°)	todo	This work
<i>F_{bol}</i> (erg cm ⁻² s ⁻¹)	todo	This work
<i>T_{eff}</i> (K)	todo	This work
<i>A_V</i> (mag)	todo	This work
<i>R</i> _★ (<i>R</i> _☉)	todo	This work
<i>L</i> _★ (<i>L</i> _☉)	todo	This work
<i>M</i> _★ (<i>M</i> _☉)	todo	This work
Age (Myr)	todo	This work

Extended Data Table 1: Properties of TIC 141146667.

137 **Acknowledgments** The author thanks X, Y, Z. L.G.B. was supported by... Acknowledge TESS...

138 **Author Contributions** ...

139 **Data Availability** ...

140 **Competing Interests** The authors declare that they have no competing financial interests.

141 **Correspondence** Correspondence and requests for materials should be addressed to ...

142 **Code availability** We provide access to a GitHub repository including all code created for the analysis of
143 this project that is not already publicly available.

144